



ARTICLE

Treatment of Agate Dyeing Wastewater Using an Immobilized Gel Mixture with Nano-Fe₃O₄ Sulfate-Reducing Bacteria

Xuying Guo^{1,*}, Guoliang Jiang², Saiou Fu³, Zhiyong Hu³, Junzhen Di², Yanrong Dong² and Ying Li⁴

¹College of Science, Liaoning Technical University, Fuxin, 123000, China

²College of Construction Engineering, Liaoning Technical University, Fuxin, 123000, China

³College of Mining Engineering, Liaoning Technical University, Fuxin, 123000, China

⁴Liaoning Fourth Geological Team Limited Liability Company, Fuxin, 123000, China

*Corresponding Author: Xuying Guo. Email: guoxuying@lntu.edu.cn

Received: 20 January 2021 Accepted: 02 March 2021

ABSTRACT

To solve the problems of high Cr⁶⁺, Cr³⁺, SO₄²⁻ and H⁺ concentrations, pollution and processing costs associated with agate dyeing industrial drainage, we prepared an immobilized gel mixture for the treatment of such drainage on the basis of microbial immobilization technology. The immobilized gel mixture was composed of sulfate-reducing bacteria (SRB), corn cob, and nano-Fe₃O₄ (nFe₃O₄). We used a single-factor experiment to determine the optimal dose of each matrix component. We analyzed the mechanism underlying the treatment of agate dyeing wastewater with an immobilized gel mixture by X-ray diffraction and scanning electron microscopy detection. The results of the single-factor test showed that the best treatment was obtained under the following conditions for each matrix component: SRB mass percentage of 30%, nFe₃O₄ dose of 3%, and corn cob mesh size of 100 and dose of 3%. On this basis, we conducted an L₉(3⁴) orthogonal experiment to determine the optimal proportion of each matrix component. The results showed that the best treatment was obtained when the gel mixture met the following conditions: SRB mass percentage of 40%, nFe₃O₄ dose of 4%, and corn cob dose of 1% and mesh size of 100. Accordingly, the SO₄²⁻, Cr⁶⁺ and Cr³⁺ removal rates from the agate dyeing drainage were 70.54%, 84.75%, and 73.80%, respectively; the total Fe and chemical oxygen demand releases were 1.086 mg·L⁻¹ and 1104 mg·L⁻¹, respectively; and the pH was 6.27. The gel mixture had the best treatment effect on agate dyeing wastewater under this composition ratio.

KEYWORDS

Agate dyeing drainage; corn cob; immobilized gel mixture; nano-Fe₃O₄; orthogonal test; sulfate-reducing bacteria

1 Introduction

A number of rural areas have developed workshop-style agate dyeing industries in Liaoning, China. Because most of the dyeing drainage is untreated and directly discharged, the local environment has become seriously polluted. Based on testing conducted by the local environmental protection department, the drainage is characterized mainly by high concentrations of hexavalent chromium and sulfate, along with strong acidity. Untreated agate dyeing drainage discharging directly into rivers and lakes pollutes water resources and poses a serious threat to drinking water sources [1]. Because of the seriously harmful



effects of acidic drainage and its relatively difficult handling, acidic drainage has become a topic of interest in relevant research fields [2]. At present, the main processing technologies used in China to treat dyeing drainage include the neutralization precipitation method [3], the wetland method [4], and the microbiological method [5]. The resultant chemical precipitate of the neutralizing precipitation method cannot be recycled and disposing of it is difficult. Furthermore, the secondary dissolution of heavy metal elements in the precipitating residue is easily triggered, which leads to new environmental problems [6]. Application of the wetland method has been restricted because of the large area of land required, the great influence on the natural environment, and the environmental pollution caused by toxic H_2S gas [7]. In biological methods, sulfate-reducing bacteria (SRB) can degrade sulfate and precipitate heavy metals by metabolizing sulfate to produce S^{2-} . The advantages of this treatment method include its strong applicability, lack of secondary pollution, and ability to recover elemental sulfur; consequently, this method has become a leading topic in the treatment of acidic drainage [8].

SRB are chemical heterotrophic microorganisms that exist widely in nature. They participate in the global sulfur cycle through dissimilatory sulfate reduction [9]. In the SRB reduction of SO_4^{2-} , adenosine triphosphate (ATP) and high-energy electrons are generated by decomposing the carbon source, which are then used to reduce SO_4^{2-} to S^{2-} and simultaneously release alkalinity. Carlier et al. [10] used an SRB-rich bioreactor to simultaneously treat wastewater from an olive oil plant and acidic mine wastewater, where the wastewater from the olive oil plant provided the carbon source and electron supply for the SRB. The resultant concentrations of pollutants such as SO_4^{2-} in the treated wastewater were below Portugal's maximum admissible values for irrigation waters. Dong et al. [11] used SRB along with coal gangue from different areas to treat acidic mine wastewater. Through dynamic leaching tests, the removal rate of SO_4^{2-} by SRB and Haizhou coal gangue was determined to be up to 72.73%. After the experiment, a contaminant release test was carried out by injecting ultrapure water. The results showed that pollutants were strongly absorbed and stabilized by the SRB and coal gangue and no secondary pollutants were released. Therefore, SRB is able to effectively metabolize SO_4^{2-} , but it requires an external carbon source and appropriate pH and environmental conditions to grow. SRB need a carbon source to grow and the cost of traditional carbon sources is high. Due to the low utilization rate of the traditional carbon source in the early stage of the reaction, most of the carbon source is lost, resulting in an insufficient carbon source in the late stage of the reaction. One solution to this problem is to use a cohesive carbon source by wrapping corn cob inside a fixed gel mixture to ensure a continuous and stable supply of carbon source for the microbes. SRB growth requires a suitable environment with an optimal pH range of 7.0–7.5 [12]. An overly acidic environment is not conducive to SRB growth, and high concentrations of heavy metals also have an inhibitory effect on their activity. Therefore, the use of an immobilized gel mixture to organically combine free SRB with a certain matrix can create a suitable microenvironment and increase the biological activity of SRB, ultimately achieving high-efficiency and low-cost acid drainage treatment.

Nano-iron series materials that are being used as new adsorption materials have the advantages of a large specific surface area, strong adsorption capacity, high reactivity, and high efficiency [13]. At present, the most commonly used nano ferric materials include nano-zero valent iron (nZVI), nano-FeS (nFeS), and nano- Fe_3O_4 (n Fe_3O_4). Jiao et al. [14] prepared activated carbon supported nZVI composites using modified activated carbon and reported the removal rate of Cr^{6+} to be more than 99%. Wang et al. [15] used nZVI synergistic SRB to treat chromium-containing wastewater, and the results showed that the removal rates of Cr^{6+} and Cr^{3+} reached 99.78% and 38.78%, respectively. However, nZVI has a high cost and is prone to surface passivation. Under the action of air and water, precipitation is promoted on the surface of nZVI, which prevents nZVI from reacting with pollutants. n Fe_3O_4 has the advantages of low cost, stable chemical properties, and good total metal adsorption performance. Liu et al. [16] used nFeS to reduce Cr(VI) to Cr(III) and attained a removal amount for Cr(VI) of $683 \text{ mg}\cdot\text{g}^{-1}$ at 15 min of reaction

by optimizing the conditions for the preparation of nFeS. However, nZVI, nFeS, and other nano-size iron materials are expensive and are prone to surface passivation. Under the action of air and water, they are prone to precipitation and other problems, which hinder further reaction between materials and pollutants. nFe₃O₄ has low cost and stable chemical properties, and exhibits good adsorption performance for heavy metal ions. Wei et al. [17] found that calcium crosslinked nFe₃O₄-modified zeolite microspheres (CA-MZs) could be prepared by modifying artificial zeolite with nFe₃O₄, which had an adsorption capacity for Cu²⁺ of up to 28.25 mg·g⁻¹. In conclusion, nFe₃O₄ is able to effectively remove heavy metal ions from wastewater, but the removal of anions such as SO₄²⁻ in agate dyeing wastewater, is difficult. At present, there are few studies on the combined use of nFe₃O₄ and SRB for the remediation of agate dyeing wastewater. nFe₃O₄ is able to remove metal ions; improve the pH of the wastewater; provide a suitable growth environment for SRB; provide reducing electrons for microorganisms [18]; promote SRB metabolism of SO₄²⁻; and achieve the synchronous restoration of SO₄²⁻, Cr⁶⁺, and Cr³⁺ in agate printing and dyeing wastewater.

Microbial fixation methods include the adsorption method, crosslinking method and embedding method, among which the embedding method has the advantages of low cost, conduciveness to substrate infiltration and product diffusion, and ability to prevent SRB leakage [19]. Therefore, we focused on the embedding method. We organically combined nFe₃O₄, corn cob, and SRB to prepare SRB immobilized gel mixtures. These gel mixtures were then used for the treatment of agate dyeing drainage. By carrying out single-factor and orthogonal experiments, we determined the optimum ratio of the four factors, SRB dose, nFe₃O₄ dose, corn cob dose, and corn cob size to prepare immobilized gel mixtures with high processing efficiency and adaptability. The introduction of nanomaterials in the preparation of the immobilized gel mixture in this experiment presented a new idea with theoretical guidance for the treatment of agate dyeing drainage.

2 Materials and Methods

2.1 Materials

We prepared the simulated dyeing wastewater used in these experiments based on the water quality characteristics measured in agate dyeing wastewater from Fuxin, Liaoning, China. The wastewater had the following constituent concentrations: pH = 4.0, c(SO₄²⁻) = 816 mg·L⁻¹, c(Cr⁶⁺) = 10 mg·L⁻¹, c(Cr³⁺) = 20 mg·L⁻¹, c(Ca²⁺) = 100 mg·L⁻¹, and c(Mg²⁺) = 50 mg·L⁻¹.

The experimental materials consisted mainly of corn cob, SRB, and nFe₃O₄. Corn cob was obtained from corn fields in the rural farmland areas of Fumeng County, Fuxin, Liaoning, China. After washing, drying, crushing, and sieving, we selected particles with 60 mesh, 100 mesh, and 200 mesh sizes. We purchased nano-size Fe₃O₄ from Beijing Deco Gold Co., Ltd., Beijing, China. SRB were extracted from 20 to 40 cm deep soil from underneath a coal gangue heap in the Xinqiu district of Fuxin City where the soil had been polluted by leach solution from the coal gangue over a long period of time. Liquid from soaking the soil sample in water was added to a sterilized Starkey medium and was enriched while in a constant temperature incubator set at 37 ± 1°C, until the SRB strain became the dominant species. After isolation and purification, we performed 16S rDNA sequencing of the strain, followed by homologous analysis using the GLOD database. The results of this analysis showed that the strain belonged to *Desulfotomaculum* and shared 98.6% similarity with *Desulfotomaculum nigrificans*. The isolated strain was named *Desulfotomaculum* Strain dz117 (referred to as dz117). We constructed a phylogenetic tree using the maximum likelihood (ML) method, as shown in Fig. 1.

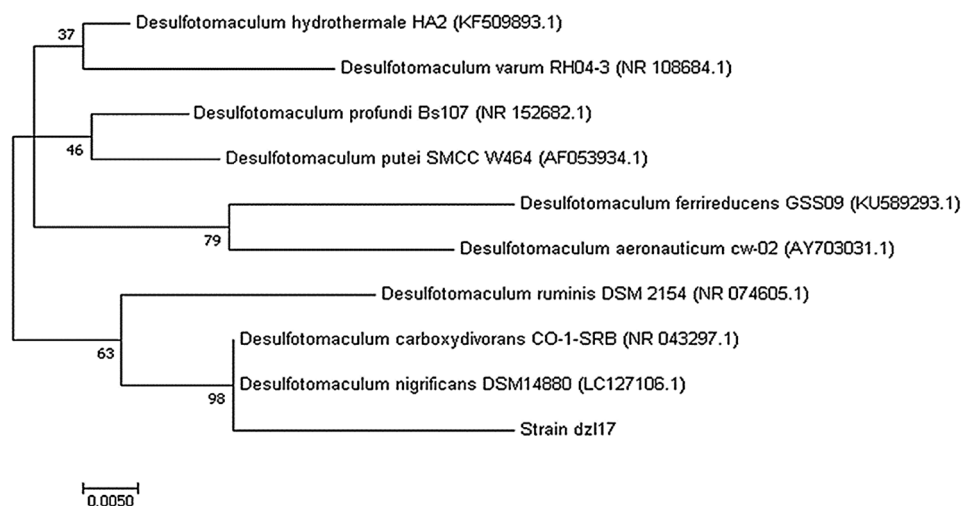


Figure 1: 16S rDNA phylogenetic tree of Strain dzl17 and desulfurized enteric bacteria

The following 16S rDNA sequence of strain dzl17 was obtained: TGGGGAATCTTCCGCAA-TGGACGAAAGCCTGACGGAGCAACGCCGCGTGAGGGAAGAAGGCCTTCGGGTTGTAAACCTC-TGTCCTAAAGGAAGAAAGAAATGACGGTACTTTAGGAGGAAGCCCCGGCTAACTACGTGCCA-GCAGCCGCGGTAAGACGTAGGGGGCAAGCGTTGTCCGGAATTACTGGGCGTAAAGGGCGCGT-AGGTGGTCCATTAAGTTAGAGGTGAAAGTGCGGGGCTTAACCCCGTTATTGCCTCTCATACTG-GTGGACTTGAGTGCTGGAGAGGGGAGTGGAAATCCCCTGTAGCGGTGAAATGCGTAGAGAT-TGGGAGGAACACTAGTGGCGAAGGCGGCTCTCTGGACTGCAACTGCACTGAGGCGCGAA-AGCGTGGGGAGCAAACAGG

2.2 Preparation of Immobilized Gel Mixture

We prepared the immobilized gel mixture based on the experimental results of previous studies conducted by our research group [20]. The weight percentage of polyvinyl alcohol (PVA) and sodium alginate was 9% and 1%, respectively, and the mass percentage was 3% for $n\text{Fe}_3\text{O}_4$ and 1%, 3%, and 5% for corn cob. The role of corn cob was to provide a carbon source, ATP, and high-energy electrons for the SRB; the role of SRB was to reduce SO_4^{2-} in the wastewater; and the role of $n\text{Fe}_3\text{O}_4$ was to adsorb heavy metal ions in the solution and provide electrons for SRB to reduce SO_4^{2-} . A beaker filled with PVA and sodium alginate was placed in a 90°C constant temperature water bath while stirring to dissolve the components until a gelatinous consistency was obtained. $n\text{Fe}_3\text{O}_4$ and corn cob with different mass fractions were added to the beaker, mixed with the gel, and then the beaker was removed from the water bath and left to cool to room temperature. Next, we added and rigorously stirred the weighed SRB to the prepared gel. Crosslinking was carried out at a rate of $100 \text{ r}\cdot\text{min}^{-1}$ using a stirrer. At the same time, the gel mixture was dropped into 2% CaCl_2 saturated boric acid using a peristaltic pump, and it was allowed to soak for 4 h before removing. The gel mixture was then rinsed repeatedly three times with 0.9% CaCl_2 solution. At this point, the gel mixture had formed a small ball with a diameter of about 4 mm, inside which SRB, corn cob, and $n\text{Fe}_3\text{O}_4$ were fixed. The surface of the ball was rich in channels and folds, which provided channels for SO_4^{2-} to enter and exit and increased the contact area with heavy metal ions.

2.3 Single-Factor Test and Orthogonal Test

We investigated the effects of SRB dose (10%, 20%, 30%, 40%, 50%), $n\text{Fe}_3\text{O}_4$ dose (1%, 2%, 3%, 4%, 5%), corn cob particle size (60 mesh, 100 mesh, 200 mesh), and corn cob dose (1%, 3%, 5%) on the removal

of chromium ions from agate dyeing wastewater by an immobilized gel mixture using a single-factor test. The prepared gel mixture was added into the wastewater with a solid-liquid ratio of 1:10, and the reaction was carried out in a constant temperature shaking table at $100 \text{ r}\cdot\text{min}^{-1}$ and 30°C . We conducted a timed sampling for five days to determine the removal rate of characteristic pollutants in the wastewater and to control the amount of pollutants released. The experiment was repeated in three groups.

On the basis of the single-factor experiment, we selected three level values to carry out an $L_9(3^4)$ orthogonal test with SRB dose, nFe_3O_4 dose, corn cob particle size, and corn cob dose as the four factors. The levels of each factor are shown in [Tab. 1](#).

Table 1: Orthogonal test factor level

Factor level	SRB dose (%)	nFe_3O_4 dose (%)	Corn cob particle size (mesh)	Corn cob dose (%)
	A	B	E	F
1	20	2	60	1
2	30	3	100	3
3	40	4	200	5

2.4 Physical and Chemical Analyses

The main parameters that were tracked in the wastewater to assess treatment effectiveness and the analytical methods used to detect them were as follows: SO_4^{2-} : barium chromate spectrophotometry (HJ/T 345-2007); Cr^{6+} : diphenylcarbazide spectrophotometry (HJ/T 342-2007); Cr^{3+} : potassium permanganate-diphenylcarbazide spectrophotometry (GB/T 7466-1987); total Fe (TFe): phenanthroline spectrophotometry (GB/T 7467-1987); COD: rapid digestion spectrophotometry (HJ/T 399-2007); and pH: glass electrode method.

3 Results and Discussion

3.1 Single-Factor Test Studies and Discussion

The experiment selected SRB dose, nFe_3O_4 dose, corn cob particle size, and corn cob dose as single factors. In [Fig. 2](#), 1#, 2#, 3#, 4#, and 5# represent SRB with mass fractions of 10%, 20%, 30%, 40%, and 50%, respectively. In [Fig. 3](#), 1#, 2#, 3#, 4#, and 5# represent nFe_3O_4 with mass fractions of 10%, 20%, 30%, 40%, and 50%, respectively. In [Fig. 4](#), 1#, 2#, and 3# indicate corn cob with respective particle sizes of 60 mesh, 100 mesh, and 200 mesh. In [Fig. 5](#), 1#, 2#, and 3# represent corn cob with mass fractions of 10%, 20%, 30%, 40%, and 50%, respectively. The main evaluation indexes were the SO_4^{2-} removal rate, Cr^{6+} removal rate, Cr^{3+} removal rate, COD release rate, and increase in pH. We determined and analyzed the optimal configuration for nFe_3O_4 treatment of agate dyeing drainage as a guide to follow up the orthogonal experimental study. The experimental results are discussed in the following section.

3.1.1 Determination of the Optimal SRB Dose

Analysis of the SO_4^{2-} Removal Effect

As shown in [Fig. 2\(a\)](#), with an increase in time, the removal rate of SO_4^{2-} gradually increased, and the removal efficiency of SO_4^{2-} was $3\# > 4\# > 2\# > 5\# > 1\#$ with the highest observed SO_4^{2-} removal rate in each case being 67.11%, 61.23%, 61.15%, 58.07%, and 52.98%, respectively. These results showed that the amount of SRB greatly influenced the activity of the strain. At the lowest dose, SRB could not efficiently metabolize SO_4^{2-} , less H^+ was consumed, and the large amount of H^+ affected the SRB growth [21], resulting in a lower SO_4^{2-} removal rate compared with the other gel mixtures. When the SRB dose was

50%, the competition between excess bacterial cells was more intense [22]. A large amount of H_2S also was produced and above a concentration of 4 mM, H_2S exerted toxic effects on SRB activity and the surrounding environment [23], which affected the SO_4^{2-} removal. The SO_4^{2-} removal rate was high in 3#, which indicated that the SRB dose used in 3# was suitable for SRB growth and reproduction in the immobilized gel mixture, resulting in higher SRB activity.

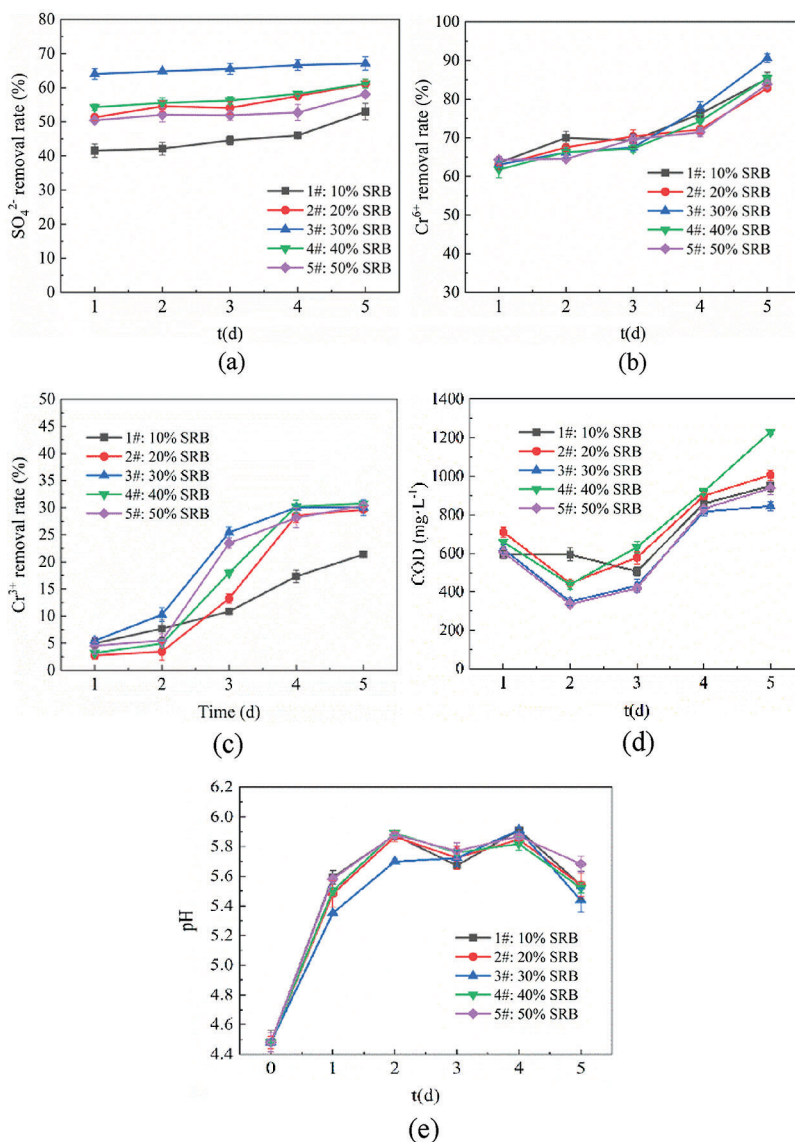


Figure 2: Test results for SRB dose: (a) SO_4^{2-} removal rate; (b) Cr^{6+} removal rate; (c) Cr^{3+} removal rate; (d) wastewater COD concentration; and (e) wastewater pH. Adapted with permission from [15], Copyright © 2021 Korean Society of Environmental Engineers

Analysis of the Cr^{6+} Removal Effect

As shown in Fig. 2(b), the removal rate of Cr^{6+} increased with time, and from high to low the removal rates were 3# > 1# > 2# > 4# > 5# with the highest rate in each case being 90.62%, 85.44%, 85.28%, 83.84%, and 82.81%, respectively. In the initial stage of the reaction, the SRB activity in the immobilized gel mixture

was weak. At this time, the number of available ATP sulfonylease, APS reductase, and sulfite reductase molecules involved in the bacterial SO_4^{2-} reduction was small [24] and the removal effect of SO_4^{2-} was not very good. The amount of free S^{2-} in the wastewater was lower, so the probability of Cr^{6+} precipitating out of solution as a metal sulfide was also greatly reduced [25], thus decreasing the Cr^{6+} removal rate. As the reaction progressed, the activity of SRB in the immobilized gel mixture increased gradually and SRB started to reduce SO_4^{2-} while producing S^{2-} and to reduce Cr^{6+} to Cr^{3+} , a process in which a large amount of Cr^{6+} was consumed. When SRB activity was high, more extracellular polymers (EPS) also were produced, which adsorbed heavy metals and increased the removal rate of Cr^{6+} . Therefore, the removal rate of Cr^{6+} increased gradually.

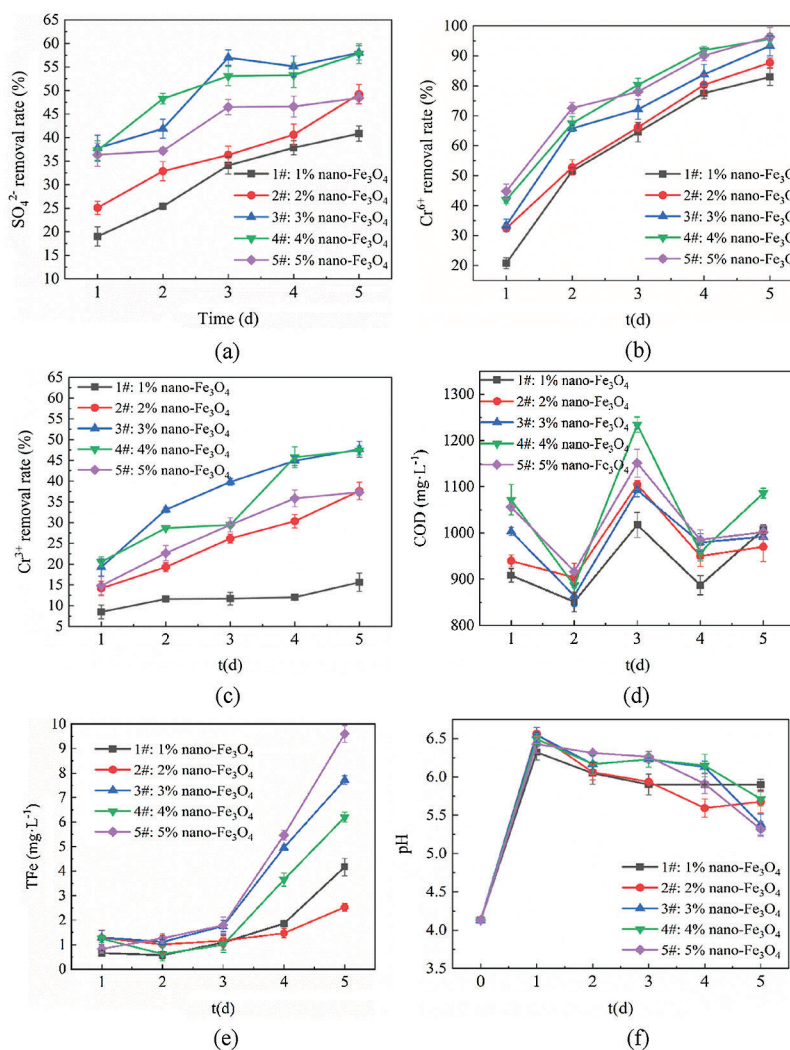


Figure 3: Test results for nFe_3O_4 dose: (a) SO_4^{2-} removal rate; (b) Cr^{6+} removal rate; (c) Cr^{3+} removal rate; (d) wastewater COD concentration; (e) amount of TFe released from the wastewater; and (f) wastewater pH

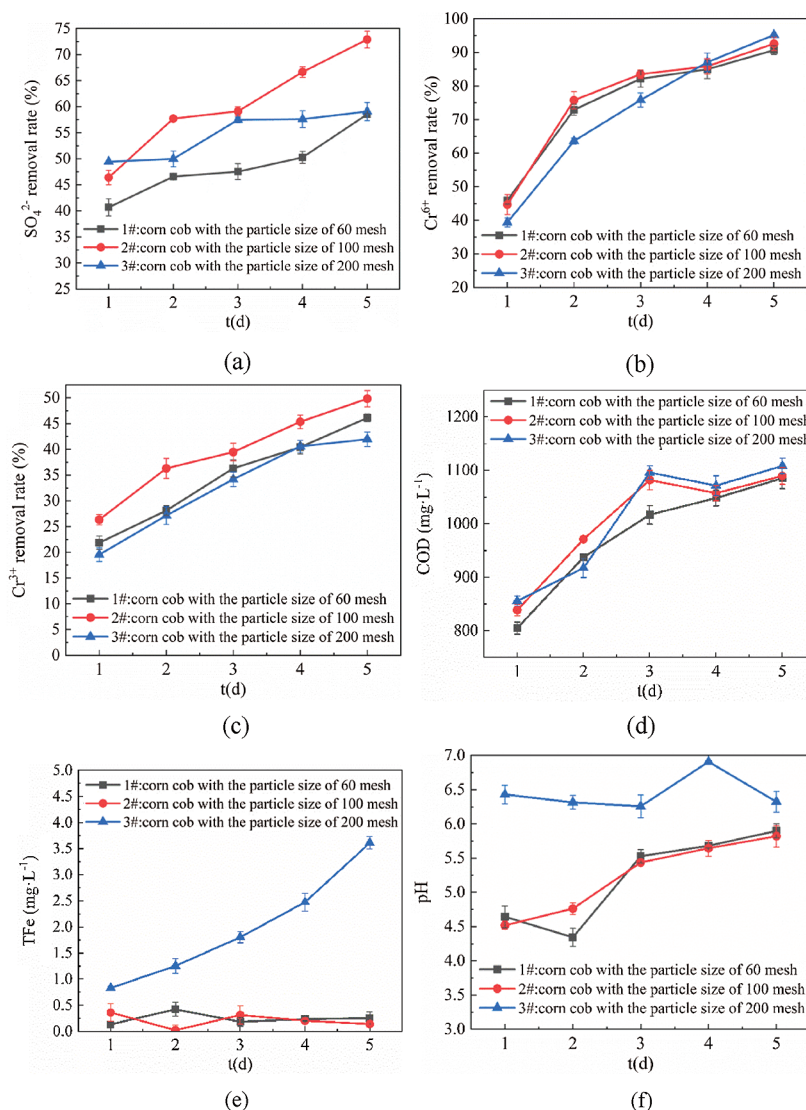


Figure 4: Test results for corn cob particle size: (a) SO_4^{2-} removal rate; (b) Cr^{6+} removal rate; (c) Cr^{3+} removal rate; (d) wastewater COD concentration; (e) amount of TFe released from the wastewater; and (f) wastewater pH

Analysis of the Cr^{3+} Removal Effect

As shown in Fig. 2(c), the removal rate of Cr^{3+} increased with time, and from high to low the removal rates were 4# > 5# > 3# > 2# > 1# with the highest rate in each case being 30.77%, 30.4%, 30.02%, 29.65%, and 21.38%, respectively. There was no obvious removal effect for Cr^{3+} because the substrate material poorly adsorbed Cr^{3+} . SRB reduced SO_4^{2-} and Cr^{6+} to S^{2-} and Cr^{3+} , respectively, and thus the concentration of Cr^{3+} increased in the wastewater [26]. Concurrently, Cr^{3+} reacted with H_2S to form Cr_2S_3 precipitate. Because the concentration of S^{2-} generated was lower than the concentration of Cr^{3+} , it was impossible to remove all of the Cr^{3+} through precipitation. Consequently, the removal effect of Cr^{3+} was not very good.

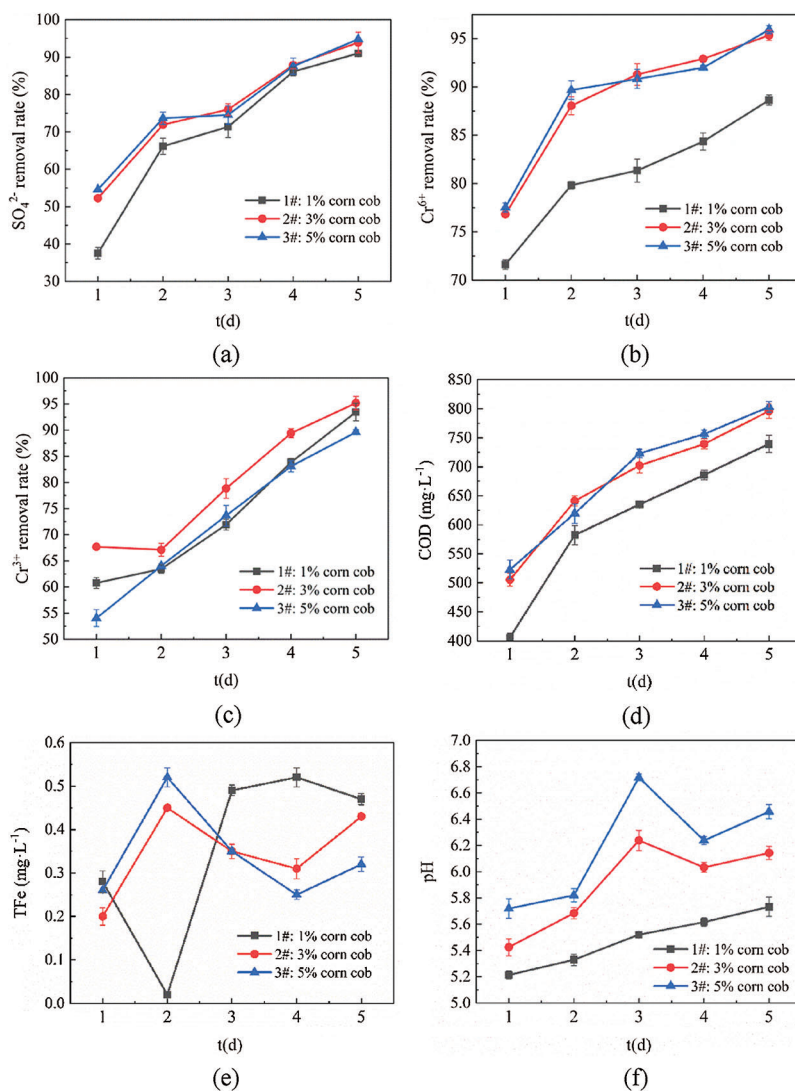


Figure 5: Test results for corn cob dose: (a) SO_4^{2-} removal rate; (b) Cr^{6+} removal rate; (c) Cr^{3+} removal rate; (d) wastewater COD concentration; (e) amount of TFe released from the wastewater; and (f) wastewater pH

Analysis of COD Release

As shown in Fig. 2(d), with an increase in time, COD release showed a fluctuating trend, and from high to low was 4# > 2# > 1# > 5# > 3#. The initial sudden increase in COD release may have been due to the rapid hydrolysis of fine particles on the surface of corn cob into organic matter [27] and the accumulation of organic matter. The decrease in COD release may have been due to the fact that the metabolic activity of reducing SO_4^{2-} with a carbon source was enhanced after the SRB flora adapted to the agate printing and dyeing wastewater environment. Therefore, the COD accumulated in the early stage was quickly consumed. The increase in COD release in the later period may have been due to the hydrolysis of larger particles of the corn cob exposed by the earlier hydrolysis of the fine particles on the surface, resulting in the release of more COD. When the COD/ SO_4^{2-} ratio was high, the available carbon sources for microorganisms were sufficient, and their metabolic activity was strong. During this time, the removal of SO_4^{2-} was improved, and the amount

of COD released was relatively high. When the number of SRB was small, the amount of COD that was used was limited, so the amount of COD remaining in the water was higher.

Analysis of the pH Value

As shown in Fig. 2(e), pH fluctuated with time and decreased slightly in the later stage of the reaction. The differences between the treatments were small, possibly because the corn cob adsorbed H^+ present in the drainage, leading to a significant increase in the pH in the early stages [28]. In the later phase of the reaction, SRB released alkaline metabolites to increase the pH [29]; however, this effect was not obvious, and the pH remained constant.

In summary, we compared the effects of an immobilized gel mixture prepared with five different SRB doses on agate printing and dyeing wastewater treatment. On the basis of the observed treatment effects, we selected 30% SRB for the follow-up orthogonal test.

3.1.2 Determination of the Optimal nFe_3O_4 Dose

Analysis of the SO_4^{2-} Removal Effect

As shown in Fig. 3(a), with time, the removal rate of SO_4^{2-} increased gradually, and the highest SO_4^{2-} removal rates were 40.85%, 49.22%, 58.01%, 57.83%, and 48.46% for 1# to 5#, respectively. The removal rate decreased in the order 3# > 4# > 2# > 5# > 1#, which indicated that adding an appropriate amount of nFe_3O_4 could promote the removal of SO_4^{2-} . At lower doses of nFe_3O_4 , the capacity to adsorb pollutants was limited, so the removal efficiency was not high. When the dose of nFe_3O_4 was too high, the biotoxicity of SO_4^{2-} could inhibit the activity of SRB [30], thus reducing the removal rate of SO_4^{2-} .

Analysis of the Cr^{6+} Removal Effect

As shown in Fig. 3(b), with time, the removal rate of Cr^{6+} increased significantly, with highest Cr^{6+} removal rates of 82.94%, 87.7%, 93.32%, 95.59%, and 96.33% for 1# to 5#, respectively. The removal rate decreased in the order 5# > 4# > 3# > 2# > 1#. As the nFe_3O_4 dose increased, its capacity to adsorb Cr^{6+} in drainage was enhanced [31], so the removal effect of Cr^{6+} became more pronounced.

Analysis of the Cr^{3+} Removal Effect

As shown in Fig. 3(c), with time, the removal rate of Cr^{3+} increased gradually, with highest Cr^{3+} removal rates of 15.63%, 37.63%, 7.67%, 47.37%, and 37.32% for 1# to 5#, respectively. The removal rate decreased in the order 3# > 4# > 2# > 5# > 1#. This indicated that nFe_3O_4 greatly influenced the adsorption of Cr^{3+} . At lower nFe_3O_4 doses, the adsorption capacity was weaker. A higher nFe_3O_4 dose would inhibit the metabolic activity of SRB, and its SO_4^{2-} metabolizing ability decreased along with the amount of S^{2-} produced, which resulted in a lower probability of precipitating Cr^{3+} and S^{2-} [32].

Analysis of COD Release

As shown in Fig. 3(d), with time, the amount of COD released showed a trend of first increasing, then falling, then increasing, and finally falling and stabilizing. The highest COD releases were 1007.22 $mg \cdot L^{-1}$, 970.3 $mg \cdot L^{-1}$, 992.02 $mg \cdot L^{-1}$, 1085.82 $mg \cdot L^{-1}$, and 1001.83 $mg \cdot L^{-1}$. The removal rate decreased in the order 4# > 1# > 5# > 3# > 2#. The sudden initial increase in COD release may have been due to the rapid hydrolysis of fine particles on the surface of the corn cob to organic matter; however, because the initial activity of the SRB flora was low and the use of organic carbon sources was limited, a large number of carbon sources accumulated. The subsequent decrease in COD release may have been due to the significant increase in SRB activity. The amount of carbon sources used also continued to increase, and thus, the COD accumulated in the early stage was rapidly consumed. The increase in COD release in the later stage may have been due to the enhanced ability of nFe_3O_4 to promote the hydrolysis of corn cobs with larger particle sizes following the hydrolysis of fine particles on the surface. Although the amount of organic

matter in the water increased significantly, the capacity for SRB utilization was limited. Because of the catalysis of $n\text{Fe}_3\text{O}_4$, most of the available organic matter in the corn cob was hydrolyzed. At this time, the hydrolysis efficiency decreased, and the amount of organic matter released was limited. Therefore, the COD content showed a decreasing trend and eventually became stable. When a large amount of nanomaterials was added to the granules, their ability to catalyze the hydrolysis of corn cobs grew stronger, so the COD release was higher. When fewer nanomaterials were added to the granules, their ability to catalyze the hydrolysis of the corn cobs was weaker, so the COD release was lower.

Analysis of TFe Release

As shown in Fig. 3(e), with time, TFe release increased continuously, and the highest TFe releases were $4.17 \text{ mg}\cdot\text{L}^{-1}$, $2.53 \text{ mg}\cdot\text{L}^{-1}$, $7.72 \text{ mg}\cdot\text{L}^{-1}$, $6.2 \text{ mg}\cdot\text{L}^{-1}$, and $9.6 \text{ mg}\cdot\text{L}^{-1}$ for 1# to 5#, respectively. TFe release decreased in the order $5\# > 3\# > 4\# > 1\# > 2\#$. This trend may have reflected the increase in the degree of hydrolysis in water as the dose of $n\text{Fe}_3\text{O}_4$ increased, which resulted in a sustained and rapid increase in the release of TFe in water during the later period of the reaction.

Analysis of pH Value

As shown in Fig. 3(f), with time, the pH showed a downward trend, and the average pH values were 5.900, 5.676, 5.379, 5.712, and 5.317. The differences among these values were small, which showed that the amount of $n\text{Fe}_3\text{O}_4$ had little influence on the pH.

Fig. 3 compares the five groups of immobilized gel mixture prepared with different $n\text{Fe}_3\text{O}_4$ dose in treating agate printing and dyeing wastewater. On the basis of the observed treatment effects, we selected 3% $n\text{Fe}_3\text{O}_4$ for use in the subsequent preparation of $n\text{Fe}_3\text{O}_4$ SRB.

3.1.3 Determination of Optimal Corn Cob Particle Size

Analysis of the SO_4^{2-} Removal Effect

As shown in Fig. 4(a), with time, the removal rate of SO_4^{2-} increased gradually, and the highest SO_4^{2-} removal rates were 58.55%, 72.9%, and 59.07% for 1# to 3#, respectively. The removal rate decreased in the order $2\# > 3\# > 1\#$. This pattern was mainly due to the excessive size of the corn cob, which could not be fully hydrolyzed in water, resulting in a low SO_4^{2-} removal rate. When the diameter of the corn cob particles was too small, the pores inside the granules were blocked, and SO_4^{2-} was not able to smoothly enter the granules for internal binding, resulting in a poor removal effect.

Analysis of the Cr^{6+} Removal Effect

As shown in Fig. 4(b), with time, the removal rate of Cr^{6+} increased significantly, and the highest Cr^{6+} removal rates were 90.67%, 92.58%, and 95.21% for 1# to 3#, respectively. The removal rate decreased in the order $3\# > 2\# > 1\#$. This pattern was mainly due to the excessive size of the corn cob, which could not be fully hydrolyzed in water [33], resulting in a low removal rate for Cr^{6+} . A decreasing corn cob particle size benefited the release of organic matter and promoted the growth of SRB. The metabolites of SRB consumed Cr^{6+} and increased the removal rate of Cr^{6+} . When the particle size of corn cob was too small, however, the pore channels inside the gel mixture were blocked, and the transfer of SRB metabolites was blocked. The remaining small amount of corn cob was not sufficient to fully adsorb Cr^{6+} , which was not conducive to the removal of Cr^{6+} .

Analysis of the Cr^{3+} Removal Effect

As shown in Fig. 4(c), with time, the removal rate of Cr^{3+} increased gradually, and the highest Cr^{3+} removal rates were 46.11%, 49.84%, and 41.96% for 1# to 3#, respectively. The removal rate decreased in the order $2\# > 1\# > 3\#$. This pattern mainly occurred because excessively large corn cob particles could not be fully hydrolyzed in water, resulting in a low Cr^{3+} removal rate. When the diameter of the

corn cob particles was too small, the pores inside the gel mixture were blocked, which inhibited the contact reaction of the gel mixture with Cr^{3+} , thus reducing the removal effect. When the grain size of corn cob was reduced properly, the SRB metabolites were in full contact with Cr^{3+} , and the removal effect of Cr^{3+} was better.

Analysis of COD Release

As shown in Fig. 4(d), with time, COD release increased significantly, and the highest amounts of COD released were $1085.2 \text{ mg}\cdot\text{L}^{-1}$, $1089.67 \text{ mg}\cdot\text{L}^{-1}$, and $1108.23 \text{ mg}\cdot\text{L}^{-1}$ for 1# to 3#, respectively. The removal rate decreased in the order $3\# > 2\# > 1\#$, suggesting that small-size corn cobs were more prone to hydrolysis in water than large-size corn cobs. Apart from the portion used by SRB, most of the remaining organic matter was accumulated and released into water.

Analysis of TFe Release

As shown in Fig. 4(e), with time, TFe release gradually increased, and the highest TFe releases were $0.250 \text{ mg}\cdot\text{L}^{-1}$, $0.142 \text{ mg}\cdot\text{L}^{-1}$, and $3.609 \text{ mg}\cdot\text{L}^{-1}$ for 1# to 3#, respectively. TFe release decreased in the order $3\# > 1\# > 2\#$. This pattern was due to the fact that as the size of the corn cob was reduced, the hydrolysis became sufficient, the generated material reacted with the nFe_3O_4 , and the Fe element was decomposed and released [34]. Consequently, the amount of TFe released tended to increase. Fe^{2+} was hydrolyzed to form floc and absorbed heavy-metal ions to form precipitates. When equilibrium between floc formation and precipitation was reached, TFe release reached its lowest level.

Analysis of the pH Value

As shown in Fig. 4(f), with time, the pH showed an upward trend, and the average pH values for 1#, 2#, and 3# were 5.897, 5.819, and 6.323, respectively. The pH decreased in the order $3\# > 1\# > 2\#$. Corn cob with a small particle size and could be fully hydrolyzed. As an absorbent material, the corn cob could better absorb the H^+ present in the water, thus causing an increase in the pH value.

In summary, we compared the effects of three different groups of immobilized corn cob particles on agate printing and dyeing wastewater. On the basis of the observed treatment effects, we selected 100 mesh corn cob for use in the subsequent preparation of nFe_3O_4 SRB.

3.1.4 Determination of Optimal Corn Cob Dose

Analysis of the SO_4^{2-} Removal Effect

As shown in Fig. 5(a), with time, the removal rate of SO_4^{2-} increased significantly. The removal rate decreased in the order $3\# > 2\# > 1\#$. This pattern may have indicated that as corn cob hydrolysis increased, the microorganisms were able to decompose more organic matter for SRB utilization. At this time, the ratio of $\text{COD}/\text{SO}_4^{2-}$ could meet the needs for the metabolic growth of microorganisms, and the activity of SRB increased correspondingly [35]. Therefore, the SO_4^{2-} removal rate increased significantly. A large dose of corn cobs resulted in greater decomposition of organic matter by hydrolyzing microorganisms in water for use by SRB. The use of organic matter by SRB was limited, however, and excessive organic matter caused secondary pollution when it entered the water. The corresponding SO_4^{2-} removal rate did not differ significantly when the corn cob doses were 3% and 5%. Therefore, we selected a corn cob mass fraction of 3%.

Analysis of the Cr^{6+} Removal Effect

As shown in Fig. 5(b), with time, the removal rate of Cr^{6+} increased significantly. The removal rate decreased in the order $3\# > 2\# > 1\#$. This pattern may have occurred because the increased hydrolysis of corn cob in water produced more organic carbon sources for SRB growth and metabolism. The resulting SRB dissociation could produce more S^{2-} for diffusion into water [36], and Cr^{6+} could combine with S^{2-}

to form metal sulfide precipitates to enhance the removal of Cr^{6+} . Consequently, the removal efficiency tended to increase. Excessive organic matter caused secondary pollution when it entered the water. The corresponding Cr^{6+} removal rate did not differ significantly when the corn cob doses were 3% and 5%. Therefore, we selected a corn cob mass fraction of 3%.

Analysis of the Cr^{3+} Removal Effect

As shown in Fig. 5(c), with time, the removal rate of Cr^{3+} increased significantly. The removal rate decreased in the order 2# > 1# > 3#. This pattern may have occurred because when the amount of corn cob increased continuously, an excessive COD/ SO_4^{2-} ratio inhibited SRB metabolic activity. At the same time, because the internal structure of the corn cob was further damaged, its ability to adsorb Cr^{3+} was reduced accordingly.

Analysis of COD Release

As shown in Fig. 5(d), with time, COD release increased significantly. The removal rate decreased in the order 3# > 2# > 1#. This pattern may have occurred because a large amount of corn cob will produce more reducing sugars and other organic substances through hydrolysis in water; however, their use by SRB was limited, resulting in a higher COD content in the effluent. Excess COD was not conducive to the growth and metabolism of SRB or the removal of SO_4^{2-} and heavy metal ions. Low COD also was not conducive to SRB metabolic activity. Therefore, we used a corn cob mass fraction of 3%.

Analysis of TFe Release

As shown in Fig. 5(e), with time, TFe release gradually increased. TFe release decreased in the order 1# > 2# > 3#. This pattern may have reflected the abundant H^+ adsorption capacity of the corn cob itself. As the corn cob dose increased, the adsorption effect for H^+ in the drainage improved, resulting in a significant increase in the pH value of the drainage. Therefore, Fe^{2+} and Fe^{3+} present in the water would form precipitates with OH^- in the water and thus be removed [37], resulting in a decrease in TFe release.

Analysis of the pH Value

As shown in Fig. 5(f), with time, the pH value gradually increased. The pH decreased in the order 3# > 2# > 1#. This pattern likely reflected the increased ability of the corn cob to absorb H^+ in the drainage as the corn cob dose increased, resulting in a significant increase in pH. This pattern also could be attributed to the increase in the number of carbon sources, which was sufficient for SRB to release alkaline molecules during the reduction process [38], resulting in an increase in pH.

In summary, we compared the effects of an immobilized gel mixture prepared with three different groups of corn cob dose on agate printing and dyeing wastewater treatment. On the basis of the observed treatment effects, we selected 3% corn cob for use in the subsequent preparation of nFe_3O_4 SRB.

3.2 Orthogonal Experimental Study

We took SRB dose, nFe_3O_4 dose, corn cob grain size, and corn cob dose as the four factors in the orthogonal test. According to the results of the single-factor test, we selected three levels. We conducted an $L_9(3^4)$ orthogonal test to determine the optimum proportion of each matrix. The experimental parameters are shown in Tab. 2.

We calculated the range and variance from Tab. 1 to determine the optimal values of SO_4^{2-} , Cr^{6+} , Cr^{3+} , COD, TFe, and pH. When the treatment was optimal, the optimal ratios of intragranular mechanisms were $\text{A}_3\text{B}_1\text{E}_1\text{F}_1$, $\text{A}_3\text{B}_3\text{E}_2\text{F}_3$, $\text{A}_1\text{B}_3\text{E}_2\text{F}_3$, $\text{A}_2\text{B}_3\text{E}_2\text{F}_1$, $\text{A}_2\text{B}_3\text{E}_2\text{F}_1$, and $\text{A}_3\text{B}_1\text{E}_2\text{F}_3$. These results confirmed that the optimal composition of nFe_3O_4 immobilized gel mixture was $\text{A}_3\text{B}_3\text{E}_2\text{F}_1$. As such, we added 40% SRB, 4% nFe_3O_4 , and 1% 100 mesh corn cob to the nFe_3O_4 immobilized gel mixture, and the performance of the gel mixture was the best under this ratio. When we added 40% SRB, 4% nFe_3O_4 , and 1% 100 mesh

corn cob, the removal rates of SO_4^{2-} , Cr^{6+} , and Cr^{3+} were 70.54%, 84.75%, and 73.80%, respectively; the releases of COD and TFe were 1104 and 1.086 $\text{mg}\cdot\text{L}^{-1}$, respectively; and the pH was 6.268. Wang et al. [15] showed that nano- Fe^0 SRB were able to immobilize the gel mixture to remove 38.78% of Cr^{3+} and 59.11% of total chromium, respectively, while the release amount of TFe was 4.26 $\text{mg}\cdot\text{L}^{-1}$ after remediation of the wastewater. Compared with these previous studies, the removal rate of total chromium and the release amount of Fe in this study were better than the noted results, translating to greater reductions in the concentrations of pollutants in wastewater.

Table 2: L_9 (3^4) experimental design and results

Test number	Factor									pH
	SRB A (%)	nFe_3O_4 B (%)	Particle size of Corn cob C (mesh)	Corn cob D (%)	Removal rate of SO_4^{2-} (%)	Removal rate of Cr^{6+} (%)	Removal rate of Cr^{3+} (%)	Release of COD ($\text{mg}\cdot\text{L}^{-1}$)	Release of TFe ($\text{mg}\cdot\text{L}^{-1}$)	
1	20	2	60	1	64.30	75.53	66.23	1077.4	0.334	6.20
2	20	3	100	3	27.49	76.50	68.22	1001.6	0.880	5.98
3	20	4	200	5	51.97	80.37	84.28	1013.2	0.130	6.09
4	30	2	100	5	23.29	81.15	72.25	1033.0	0.036	6.02
5	30	3	200	1	22.17	77.34	57.80	1058.8	0.512	5.14
6	30	4	60	3	21.16	79.91	67.63	1044.2	1.052	5.21
7	40	2	200	3	61.35	80.67	56.51	1006.8	0.316	6.08
8	40	3	60	5	53.65	83.65	58.96	955.0	0.038	6.30
9	40	4	100	1	70.54	84.75	73.80	1104.0	1.086	6.27

3.3 Gel Mixture Characterization

3.3.1 X-ray Diffraction Analysis

We prepared immobilized gel mixtures to treat agate dyeing wastewater according to the optimal ratio determined by the orthogonal experiment. The gel mixture before and after the reaction was dried at 60°C and ground to 200 mesh. We analyzed the phase of the elements contained in the gel mixture before and after the reaction by X-ray diffraction (XRD). The results of the analysis are shown in Figs. 6(a) and 6(b).

Figs. 6(a) and 6(b) are the XRD analysis diagrams of the immobilized gel mixture before and after the reaction, respectively. Fig. 6(a) shows that the Fe element in the gel mixture before the reaction was in the form of Fe_3O_4 and Fe_2O_3 , and that the gel also contained organic matter $\text{C}_{12}\text{H}_8\text{O}_4$. The main components of the gel mixture were nFe_3O_4 and corn cob materials, and a portion of Fe_3O_4 exposed to air at the surface was oxidized into Fe_2O_3 . Fig. 6(b) shows that the two Fe phases Fe_3O_4 and Fe_2O_3 disappeared from the gel mixture after the reaction, and two new compounds, Cr_2S_3 and FeS , appeared simultaneously. nFe_3O_4 , SRB, and corn cob were fixed inside the gel mixture. When the gel mixture was placed into the wastewater, the SRB inside the gel mixture first decomposed the corn cob to provide ATP and high-energy electrons for itself, and generated water, CO_2 and organic acids. SRB used ATP and high-energy electrons to reduce SO_4^{2-} , Cr^{6+} , and Fe_3O_4 to H_2S , Cr^{3+} , and Fe^{2+} , respectively, after which Cr^{3+} and Fe^{2+} in the wastewater could combine with S^{2-} to form metal sulfide precipitates. After the reaction, the organic components disappeared, indicating that the corn cob was completely decomposed by SRB. The resulting organic acids entered the wastewater through the gel mixture channel.

3.3.2 Scanning Electron Microscopy Analysis

The immobilized gel mixture before and after the reaction was dried at 60°C and characterized by scanning electron microscopy (SEM) 200 times to explore the reaction process and related removal mechanism of the gel mixture, as shown in Figs. 6(c) and 6(d).

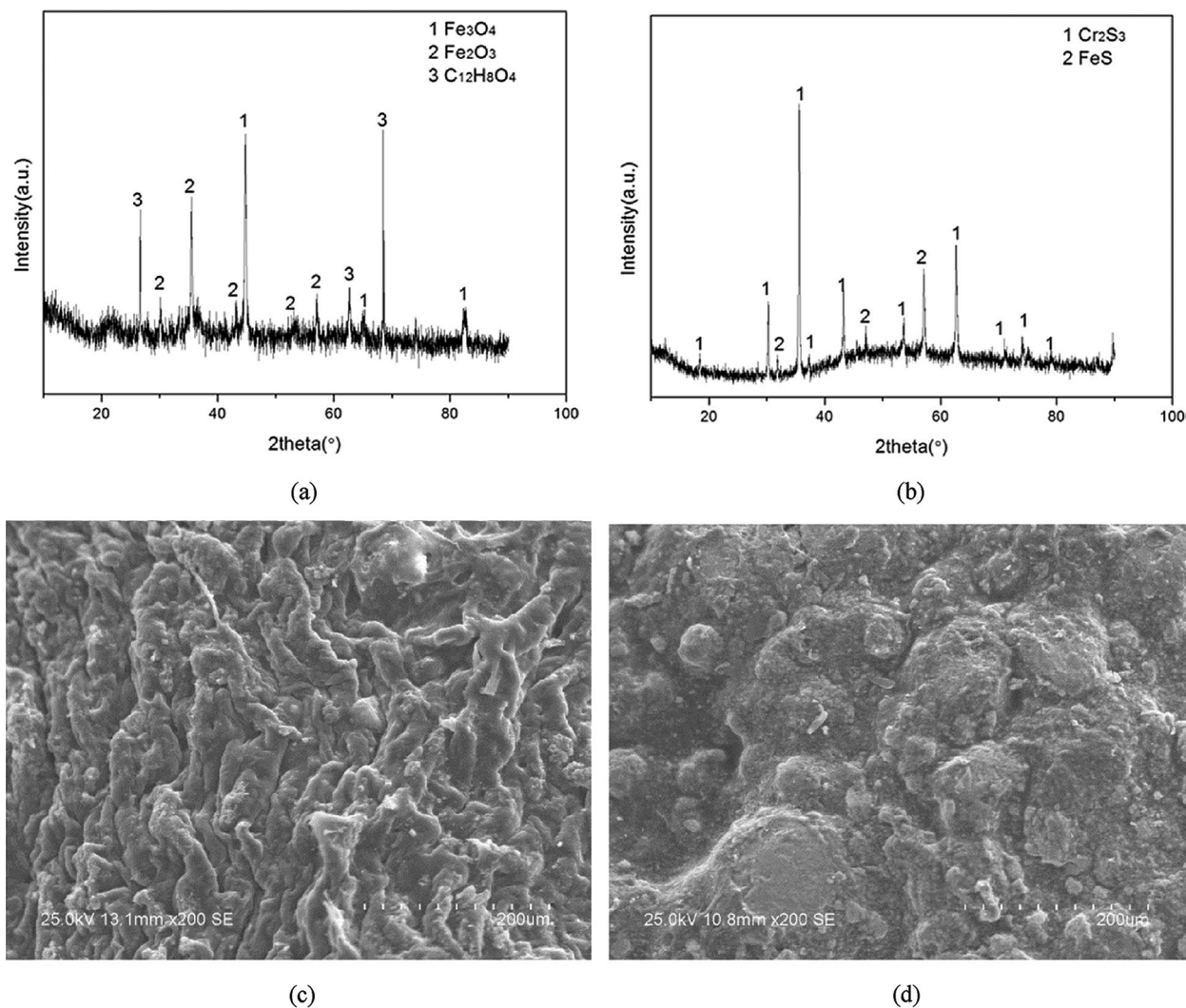


Figure 6: Particle XRD and SEM analysis: (a) XRD diagram before particle treatment of wastewater. (b) XRD diagram after particle treatment of wastewater. (c) SEM diagram before particle treatment of wastewater. (d) SEM diagram after particle treatment of wastewater

As shown in Figs. 6(c) and 6(d), the surface of the gel mixture before the reaction presented a multi-cross strip-like fold structure, but after the reaction, large spherical folds appeared on the surface of the gel mixture, and a large amount of sediment was obviously visible on the surface. The gel mixture was internally fixed with $n\text{Fe}_3\text{O}_4$, so the gel mixture had a certain adsorption capacity for heavy metals. When it was put into the wastewater, the chromium ions in the wastewater adsorbed to the surface of the gel mixture. The chromium ions on the surface inhibited SRB activity and caused the surface folding structure to change. At the same time, S^{2-} generated by SRB reacted with Cr^{3+} and Fe^{2+} in the wastewater, and the resultant FeS and Cr_2S_3 precipitates were adsorbed onto the surface of the gel mixture, resulting in an obvious gel mixture deposition.

4 Research Implications

A large amount of dyeing wastewater is produced in the production of agate. The field research has found that the dyeing wastewater contains large amounts of SO_4^{2-} , Cr^{6+} and Cr^{3+} , which causes serious

damage to the surrounding environment. As traditional water treatment technologies fail to treat dyeing wastewater effectively in practical application, the study leverages immobilization technology to combine $n\text{Fe}_3\text{O}_4$, SRB and corncob to treat dyeing wastewater. The author analyzed the influence of factors including SRB, $n\text{Fe}_3\text{O}_4$, corncob volume and corncob size on treatment of dyeing wastewater with immobilized gel mixture based on the change of pollutant index in the system as well as XRD and SEM techniques, revealing the mechanism of action of immobilized gel mixture in treating dyeing wastewater. This study can not only break the bottleneck that SO_4^{2-} in dyeing wastewater is difficult to be removed with $n\text{Fe}_3\text{O}_4$, but also resolve the problems that low pH and heavy metal ions are insufficient to inhibit the SRB activity and supply carbon sources, so as to ensure that the advantages of $n\text{Fe}_3\text{O}_4$ and SRB can be maximized in the treatment of agate dyeing wastewater. The introduction of $n\text{Fe}_3\text{O}_4$ in the preparation of the immobilized gel mixture in this experiment presented a new idea with theoretical guidance for the treatment of agate dyeing drainage.

5 Conclusions

On the basis of this study, the following conclusions can be drawn:

1. Through a single-factor test, it is determined that the optimum dosage of SRB is 30%, the optimum dosage of $n\text{Fe}_3\text{O}_4$ is 3%, the optimum particle size of corncob is 100 mesh, and the optimum dosage of corncob is 3%.
2. Through the orthogonal test, we determined that the optimal composition of the $n\text{Fe}_3\text{O}_4$ immobilized gel mixture was 40% SRB, 4% $n\text{Fe}_3\text{O}_4$, and 1% 100 mesh corn cob. Accordingly, the SO_4^{2-} , Cr^{6+} and Cr^{3+} removal rates from the agate dyeing drainage were 70.54%, 84.75%, and 73.80%, respectively; the total Fe and chemical oxygen demand releases were $1.086 \text{ mg}\cdot\text{L}^{-1}$ and $1104 \text{ mg}\cdot\text{L}^{-1}$.
3. Through the XRD analysis, the elements Cr and S appeared in the immobilized gel mixture following the reaction in the form of Cr_2S_3 and FeS phases. SEM analysis showed that the surface structure of the gel mixture changed before and after the reaction, and FeS and Cr_2S_3 deposits were adsorbed onto the surface of the gel mixture.

Acknowledgement: We thank LetPub (www.letpub.com) for its linguistic assistance during the preparation of this manuscript.

Funding Statement: The project was funded by the National Natural Science Foundation of China (41672247, 41102157, 51304114), Liaoning Provincial Natural Science Foundation of China (2015020619), and Liaoning Provincial Department of Education (LJYL031, LJ2017FAL016), and the project was supported by the discipline innovation team of Liaoning Technical University (LNTU20TD-21).

Conflicts of Interest: The authors declare that they have no conflicts of interest to report regarding the present study.

References

1. Kefeni, K. K., Msagati, T. A. M., Mamba, B. B. (2017). Acid mine drainage: Prevention, treatment options, and resource recovery: A review. *Journal of Cleaner Production*, 151, 475–493. DOI 10.1016/j.jclepro.2017.03.082.
2. Qureshi, A., Jia, Y., Maurice, C., Öhlander, B. (2016). Potential of fly ash for neutralisation of acid mine drainage. *Environmental Science and Pollution Research*, 23(17), 17083–17094. DOI 10.1007/s11356-016-6862-3.
3. Peiravi, M., Mote, S. R., Mohanty, M. K., Liu, J. (2017). Bioelectrochemical treatment of acid mine drainage (AMD) from an abandoned coal mine under aerobic condition. *Journal of Hazardous Materials*, 333(209), 329–338. DOI 10.1016/j.jhazmat.2017.03.045.
4. Riato, L., Leira, M., Bella, V. D., Oberholster, P. J. (2018). Development of a diatom-based multimetric index for acid mine drainage impacted depressional wetlands. *Science of the Total Environment*, 612, 214–222. DOI 10.1016/j.scitotenv.2017.08.181.

5. Kaur, G., Couperthwaite, S. J., Hatton-Jones, B. W., Millar, G. J. (2018). Alternative neutralisation materials for acid mine drainage treatment. *Journal of Water Process Engineering*, 22, 46–58. DOI 10.1016/j.jwpe.2018.01.004.
6. Tyagi, S., Malik, W., Annachhatre, A. P. (2020). Heavy metal precipitation from sulfide produced from anaerobic sulfidogenic reactor. *Materials Today: Proceedings*, 32(1–2), 936–942. DOI 10.1016/j.matpr.2020.05.076.
7. Oberholster, P. J., Klerk, A. R. D., Klerk, L. D., Chamier, J., Botha, A. (2016). Algal assemblage responses to acid mine drainage and steel plant wastewater effluent up and downstream of pre and post wetland rehabilitation. *Ecological Indicators*, 62(10), 106–116. DOI 10.1016/j.ecolind.2015.11.025.
8. Dong, Y., Di, J., Yang, Z., Wang, X., Zhang, J. (2020). Repairing effects of sulfate-reducing bacteria on the dissolved pollutant of coal gangue based on leaching experiments. *Energy Sources Part A: Recovery Utilization and Environmental Effects*, 38, 1–14. DOI 10.1080/15567036.2020.1738598.
9. Daryna, A., Jozef, K., Galyna, I., Ivan, K. (2020). ATP sulfurylase activity of sulfate-reducing bacteria from various ecotopes. *3 Biotech*, 10(2), 178. DOI 10.1007/s13205-019-2041-9.
10. Carlier, J. D., Luís, A. T., Alexandre, L. M., Costa, M. C. (2020). Feasibility of co-treating olive mill wastewater and acid mine drainage. *Mine Water and the Environment*, 39(4), 1–22. DOI 10.1007/s10230-020-00719-1.
11. Dong, Y., Di, J., Yang, Z., Wang, X., Guo, X. et al. (2020). Study on the effectiveness of sulfate-reducing bacteria combined with coal gangue in repairing acid mine drainage containing Fe and Mn. *Energies*, 13(4), 1–21. DOI 10.3390/en13040995.
12. Kikot, P., Viera, M., Mignone, C., Dontail, E. R. (2009). Isolation of mesophilic sulphate-reducing bacteria from a microbial community: Comparative study of the effect of pH and dissolved heavy metals on the reduction of sulphate. *Advanced Materials Research*, 835, 549–552. DOI 10.4028/www.scientific.net/AMR.71-73.549.
13. Sahoo, P. K., Equeenuddin, S. M., Powell, M. A. (2016). Trace elements in soils around coal mines: Current scenario, impact and available techniques for management. *Current Pollution Reports*, 2(1), 1–14. DOI 10.1007/s40726-016-0025-5.
14. Jiao, C., Tan, X., Lin, A., Yang, W. (2020). Preparation of activated carbon supported bead string structure nano zero valent iron in a polyethylene glycol-aqueous solution and its efficient treatment of Cr(VI) wastewater. *Molecules*, 25(1), 1–15. DOI 10.3390/molecules25184052.
15. Wang, X., Di, J., Liang, B., Yang, W., Dong, Y. et al. (2020). Study on treatment of acid mine drainage by nano zero-valent iron synergistic with SRB immobilized particles. *Environmental Engineering Research*, 26(5), 1–13. DOI 10.4491/eer.2020.333.
16. Liu, Y., Xiao, W., Wang, J., Mirza, Z. A., Wang, T. (2016). Optimized synthesis of FeS nanoparticles with a high Cr (VI) removal capability. *Journal of Nanomaterials*, 2016(4), 1–9. DOI 10.1155/2016/7817296.
17. Wei, J., Long, X., Wang, J., Tang, Z., Wang, T. et al. (2021). Preparation of calcium cross-linked nano-Fe₃O₄ modified zeolite microspheres for Cu²⁺ adsorption from wastewater. *Journal of Wuhan University of Technology (Materials Science)*, 35(6), 1021–1030. DOI 10.1007/s11595-020-2351-0.
18. Romano, P. (2018). Experiences in hexavalent chromium removal in the treatment of drinking water. *Italian Water Industry*, 2018, 101–117. DOI 10.1007/978-3-319-71336-6.
19. Yang, J., Huang, Y., Wu, C., Cai, X. (2006). The influence of temperature and pH on the activity of SRB. *Journal of Maoming College*, 16(4), 1–3. DOI 10.3969/j.issn.2095-2562.2006.04.001.
20. Korak, J. A., Huggins, R., Arias-Paic, M. (2017). Regeneration of pilot-scale ion exchange columns for hexavalent chromium removal. *Water Research*, 118(5), 141–151. DOI 10.1016/j.watres.2017.03.018.
21. Gil-Garcia, C., Godoi, L. A. G. D., Fuess, L. T., Damianovic, M. H. R. Z. (2018). Performance improvement of a thermophilic sulfate-reducing bioreactor under acidogenic conditions: Effects of diversified operating strategies. *Journal of Environmental Management*, 207, 303–312. DOI 10.1016/j.jenvman.2017.11.043.
22. Subhabrata, D., Shantonu, R., Jayanta, B. (2016). Understanding the performance of sulfate reducing bacteria based packed bed reactor by growth kinetics study and microbial profiling. *Journal of Environmental Management*, 177, 101–110. DOI 10.1016/j.jenvman.2016.03.049.
23. Ivan, K., Dani, D., Monika, V. (2019). Toxicity of hydrogen sulfide toward sulfate-reducing bacteria *Desulfovibrio piger* Vib-7. *Archives of Microbiology*, 201(3), 389–397. DOI 10.1007/s00203-019-01625-z.

24. Ivan, K., Daryna, A., Jozef, K., Dani, D., Monika, V. (2020). Adenosine-5'-phosphosulfate- and sulfite reductases activities of sulfate-reducing bacteria from various environments. *Biomolecules*, 912(10), 1–15. DOI 10.3390/biom10060921.
25. Tang, J. H., Xu, G. R., Li, G. B., Spinosa, L. (2011). Adsorption properties of chromium (VI) on extracellular polymeric substances (EPS), Lushan, China. *International Conference on Electric Technology & Civil Engineering*, 983–986. DOI 10.1109/icetce.2011.5776119.
26. Fuller, S. J., Burke, I. T., McMillan, D. G. G., Ding, W., Stewart, D. I. (2015). Population changes in a community of alkaliphilic iron-reducing bacteria due to changes in the electron acceptor: Implications for bioremediation at alkaline Cr(VI)-contaminated sites. *Water, Air, & Soil Pollution*, 226(6), 180. DOI 10.1007/s11270-015-2437-z.
27. Lin, H., Han, S., Dong, Y., Ling, W., He, Y. (2018). Structural characteristics and functional properties of corn cob modified by hyperbranched polyamide for the adsorption of Cr (VI). *Water Air & Soil Pollution*, 229(4), 1–12. DOI 10.1007/s11270-017-3647-3.
28. Cai, C. F., Qi, F. Z., Lin, X. L., Jiang, L. (2014). Treatment of simulated acid mine drainage by permeable reactive barrier: Column study. *Advanced Materials Research*, 3326, 966–969. DOI 10.4028/www.scientific.net/AMR.989-994.966.
29. Gallagher, K. L., Kading, T. J., Braissant, O., Dupraz, C., Visscher, P. T. (2012). Inside the alkalinity engine: The role of electron donors in the organomineralization potential of sulfate-reducing bacteria. *Geobiology*, 10(6), 518–530. DOI 10.1111/j.1472-4669.2012.00342.x.
30. Katsnelson, B. A., Degtyareva, T. D., Minigalieva, I. I., Privalova, L. I., Kuzmin, S. V. et al. (2011). Subchronic systemic toxicity and bioaccumulation of Fe₃O₄ nano- and microparticles following repeated intraperitoneal administration to rats. *International Journal of Toxicology*, 30(1), 59–68. DOI 10.1177/1091581810385149.
31. Shen, H., Pan, S., Zhang, Y., Huang, X., Gong, H. (2012). A new insight on the adsorption mechanism of amino-functionalized nano-Fe₃O₄, magnetic polymers in Cu(II), Cr(VI) co-existing water system. *Industrial Crops and Products*, 183, 180–191. DOI 10.1016/j.cej.2011.12.055.
32. Bai, H., Kang, Y., Quan, H. E., Han, Y., Feng, Y. (2012). Treatment of copper drainage by sulfate reducing bacteria in the presence of zero valent iron. *International Journal of Mineral Processing*, 112–113, 71–76. DOI 10.1016/j.minpro.2012.06.004.
33. Wang, C. J., Tang, L. L., Zou, Z., Liu, W. J., Xie, J. et al. (2013). Experimental study on Cr⁶⁺ adsorption in water about Corn cob. *Advanced Materials Research*, 652–654, 1656–1659. DOI 10.4028/www.scientific.net/AMR.652-654.1656.
34. Silvério, H. A., Neto, W. P. F., Dantas, N. O., Pasquini, D. (2013). Extraction and characterization of cellulose nanocrystals from corn cob for application as reinforcing agent in nanocomposites. *Industrial Crops and Products*, 44(12), 427–436. DOI 10.1016/j.indcrop.2012.10.014.
35. Zhou, L. J., Zhuang, W. Q., Wang, X., Yu, K., Yang, S. F. et al. (2017). Potential effects of loading nano zero valent iron discharged on membrane fouling in an anoxic/oxic membrane bioreactor. *Water Research*, 111(1), 140–146. DOI 10.1016/j.watres.2017.01.007.
36. Lu, Z. F., Wang, H. M., Li, J. Y., Yuan, L. X., Zhu, L. W. (2015). Adsorption characteristics of bio-adsorbent on chromium(III) in industrial drainage. *Water Science and Technology*, 72(7), 1051–1061. DOI 10.2166/wst.2015.237.
37. Liu, R. H., Deng, S., Chen, J. W., Jiang, B. H. (2014). Method of modified corn cob adsorbing heavy metal ions from water. *Advanced Materials Research*, 955–959, 2458–2462. DOI 10.4028/www.scientific.net/AMR.955-959.2458.
38. Rajalakshmi, N., Sarada, B. Y., Dhathathreyan, K. S. (2015). Porous carbon nanomaterial from corn cob as hydrogen storage material. *Advanced Porous Materials*, 2(3), 165–170. DOI 10.1166/apm.2014.1068.